



Universitat de Lleida

Document downloaded from:

<http://hdl.handle.net/10459.1/59860>

The final publication is available at:

<https://doi.org/10.1016/j.solmat.2017.05.036>

Copyright

cc-by-nc-nd, (c) Elsevier, 2017



Està subjecte a una llicència de [Reconeixement-NoComercial-SenseObraDerivada 4.0 de Creative Commons](https://creativecommons.org/licenses/by-nc-nd/4.0/)

Characterization of wastes based on inorganic double salt hydrates as potential thermal energy storage materials

Andrea Gutierrez¹, Svetlana Ushak^{1*}, Veronica Mamani¹, Pedro Vargas¹, Camila Barreneche^{2,3},
Luisa F. Cabeza², Mario Grágeda¹

¹Department of Chemical Engineering and Mineral Processing and Center for Advanced Study of Lithium and Industrial Minerals (CELiMIN), Universidad de Antofagasta, Campus Coloso, Av. Universidad de Antofagasta 02800, Antofagasta, Chile.

²GREIA Innovació Concurrent, Edifici CREA, Universitat de Lleida, Pere de Cabrera s/n, Lleida 25001, Spain

³ Department of Materials Science & Physical Chemistry, Universitat de Barcelona, Martí i Franqués 1, 08028, Barcelona

Corresponding author: svetlana.ushak@uantof.cl

Abstract

Thermal energy storage (TES) is seen today as a key technology to reduce the existing gap between energy demand and energy supply in many energy systems. There are, currently, three well known methods to store thermal energy and they are: sensible heat storage (SHS), latent heat storage (LHT) and thermochemical heat storage. Every method has its own thermophysical requirements for the mediums of storage, such as thermal stability, high enthalpy of phase change or reaction, high heat capacity and suitable temperature of the thermal phenomenon for a respective application, among others. In this regard, the composition of materials usually needs to be modified in order to improve their performance or to reach a determined requirement. As a consequence, the costs of potential TES materials to be applied in renewable energy systems are too high to compete with traditional systems using fossil fuels. On the other hand, several wastes and by-products from the non-metallic mining, such as salt hydrates and double salts, are available without any application but accumulating in the mining sites. This is the case for astrakanite ($\text{Na}_2\text{SO}_4 \cdot \text{MgSO}_4 \cdot 4\text{H}_2\text{O}$) and lithium carnallite ($\text{LiCl} \cdot \text{MgCl}_2 \cdot 7\text{H}_2\text{O}$) with no current application, and potassium carnallite ($\text{KCl} \cdot \text{MgCl}_2 \cdot 6\text{H}_2\text{O}$) used as a supplementary raw material to obtain KCl. Since the costs of these materials are close to zero, they were characterized as TES materials taking into account the properties required for the three methods of storage. Results showed that astrakanite and potassium carnallite have potential to be applied as thermochemical material at low-medium temperature ($<300^\circ\text{C}$). Also, a dehydrated product obtained from astrakanite showed potential to be applied as phase change material (PCM) at high temperature, from 550°C to 750°C . Nevertheless, lithium

carnallite did not show potential to be applied as TES material due to its low thermal stability, presenting partial decomposition below 200°C.

Keywords: Thermal Energy Storage; Salt Hydrates; Waste Materials; Double Salts

Nomenclature

TES	Thermal Energy Storage	-
SHS	Sensible Heat Storage	-
LHS	Latent Heat Storage	-
PCM	Phase Change Material	-
TCM	Thermochemical Material	-
SEM	Scanning Electron Microscope	-
EDX	Energy dispersive X-ray spectrometer	-
TG	Thermogravimetry	-
MS	Mass Spectrometer	-
DSC	Differential Scanning Calorimetry	-
HT	High Temperature	-
XRD	X-Ray Diffraction	-
HR	Heating rate	K/min
Q_{sensible}	Sensible Heat	J/g
Q_{latent}	Latent Heat	J/g
c_p	Heat Capacity	J/g K
T	Temperature	°C
T_{onset}	Onset temperature	°C
$\Delta_F H$	Enthalpy of Fusion	J/g
$\Delta_S H$	Enthalpy of Solidification	J/g
$\Delta_D H$	Enthalpy of Dehydration	J/g
$\Delta_H H$	Enthalpy of Hydration	J/g
wt. %	Percentage of weight loss	%

1. Introduction

Thermal energy storage (TES) is seen today as a key technology to reduce the existing gap between energy demand and energy supply in many energy systems [1, 2].

There are three well known methods to store energy and they are detailed below:

1.1 Sensible heat storage (SHS)

1.2

The first and most studied method up to date is the SHS. This is the amount of energy involved to increase or decrease the temperature of a substance without experiencing a phase change [3]. It is calculated with following Eq. 1:

$$Q_{sensible} = \int_{T_1}^{T_2} c_p \cdot dT \quad \text{Eq. 1}$$

As can be seen in Eq. 1 $Q_{sensible}$ strongly depends on the c_p of the material. The themophysical requirements of materials for SHS are divided and listed in two main groups:

1.2.1 Physical and technical requirements:

- High density
- Temperature range fitted to the application
- High cyclic stability
- Large scale production methods
- Non-corrosive
- Low system complexity
- Low vapor pressure in the temperature range

1.2.2 Thermal requirements:

- High energy density
- High thermal conductivity
- Low thermal diffusivity
- Good specific heat capacity
- Thermal expansion coefficient

These requirements are defined most of the time based on the application conditions. Once this is established, it starts the searching of materials that address the majority of the requirements. While all the mentioned properties are important, Fernandez et al. [4] determined that the thermal requirements are the most significant, reporting as well the merit index of such material to be used

to store sensible heat. In addition, the energy density is one of the most significant property. For the SHS materials, the theoretical energy density can be calculated multiplying the c_p by the density of the material.

1.3 Latent Heat Storage (LHS)

The second method of storage is LHS which is used when a higher energy density, compared to SHS, is required in a given application [3]. The solid to liquid phase change is chosen most of the time in order to avoid technical issues. The energy stored for this method is calculated as follows:

$$Q_{latent} = \int_{T_1}^{T_{pc}} c_{p,s} \cdot dT + \Delta H_{pc} + \int_{T_{pc}}^{T_2} c_{p,l} \cdot dT \quad \text{Eq. 2}$$

In this case, the materials used are known as phase change materials (PCM) [5], and the constant temperature of the phase change is taken as an advantage in their application. The requirements of the materials for LHS are divided in the same two groups as before [6]:

1.3.1 Physical and technical requirements:

- Low density variation and small volume change
- High energy density
- Small or no subcooling
- No phase segregation
- Low vapor temperature
- Chemical and physical stability
- Compatible with other materials

1.3.2 Thermal requirements:

- Suitable phase change temperature fitted to application
- Large enthalpy of phase change ($\Delta_F H$ and $\Delta_S H$) and specific heat (c_p)
- High thermal conductivity (except for passive cooling)
- Reproducible phase change
- Thermal stability
- Cycling stability

In this case, Barreneche et al. [7] determined the merit index to select the best candidate to be used as PCM., where the database reported considers the main thermal properties required for it. That is, the phase change enthalpy, ΔH_{pc} and the energy density of potential materials.

1.4 Thermochemical Energy Storage

1.5

The last method to store energy is thermochemical energy storage, where the energy stored is produced by a reversible chemical reaction or during a sorption process. Usually, solid-gas reactions are considered, due to the technical advantages of separating a gas from a solid to store the materials (products of reaction), and later combination in order to start the inverse reaction. The materials used to store thermochemical energy are known as thermochemical materials (TCM). The requirements of the materials for thermochemical energy storage are divided in the two groups as well [8]:

1.5.1 Physical and technical requirements:

- Low density and small volume change
- High energy density
- No phase segregation
- Chemical and physical stability
- Compatible with other materials - Non-corrosive

1.5.2 Thermal requirements:

- Reversible reaction
- Control of the kinetic model
- Control of the structure changes
- Water stability within crystal structure (For salt hydrate and hydroxide systems)
- Proper particle size
- Control of the impurities
- Solubility of the TCM in the working conditions (P, T)
- Suitable working temperature range fitted to the application
- Large energy involved in the reaction ($\Delta_D H$ and $\Delta_H H$ for Salt hydrate and hydroxide systems)
- High thermal conductivity
- Thermal stability
- Cycling stability

Notice that TCM have more extensive technical requirements than PCM or SHS materials. Additionally, TCM takes into account chemical transformation and not only physical transformation like the other two types of materials, this makes the application of TCM more challenging from the technical and scientific point of view. This results from the fact that activation energy of chemical reactions strongly depends on temperature and pressure [9]. As a consequence, the results obtained

for the same material can vary when these two variables are modified [10]. However, the significant high energy storage density of TCM (quantified as 10 time higher than SHS density) has increased the motivation to study these materials [11].

1.6 Inorganic wastes studied as storage medium for TES

1.7

The use of by-products or waste materials to store thermal energy is becoming a promising option to be used as TES materials due to their low-cost, close to zero, as was stated by Gutierrez et al. [12]. In addition, Chile is an important non-metallic mining producer obtaining more than 60,646 ton of lithium compounds, 1,901,215 ton of potassium compounds, 6,576,960 ton of sodium chloride and 759,384 ton of nitrates among others every year [13]. In previous studies, bischofite was characterized and results showed that this by-product has a high potential to be used as PCM for TES at low temperature ($\sim 100^{\circ}\text{C}$) [14].

Since the salt production process is complex, tons of by-products and several wastes are obtained every year, for example, astrakanite ($\text{Na}_2\text{SO}_4 \cdot \text{MgSO}_4 \cdot 4\text{H}_2\text{O}$), potassium carnallite ($\text{KCl} \cdot \text{MgCl}_2 \cdot 6\text{H}_2\text{O}$) and lithium carnallite ($\text{LiCl} \cdot \text{MgCl}_2 \cdot 7\text{H}_2\text{O}$), among others. As most of these by-products and wastes don't have any application they must be just landfilled. Consequently, finding an alternative application in order to valorize these salts, besides of the reduction of the accumulation of wastes, it is currently an important topic of study [15]. Therefore, their potential implementation as TES materials is a key issue for the sustainability of mining processes in Chile and in the salt producers' countries worldwide. What is more, evaluating the potential of these cost-effective materials could increase the suitability of new technologies to produce heat and/or electricity using renewable energy sources.

The main goal of this study is to evaluate the potential of astrakanite ($\text{Na}_2\text{SO}_4 \cdot \text{MgSO}_4 \cdot 4\text{H}_2\text{O}$), potassium carnallite ($\text{KCl} \cdot \text{MgCl}_2 \cdot 6\text{H}_2\text{O}$), and lithium carnallite ($\text{LiCl} \cdot \text{MgCl}_2 \cdot 7\text{H}_2\text{O}$), three by-products or wastes from the non-metallic industry, as TES material candidates to be implemented considering the three different methods to store thermal energy; sensible TES, latent TES and thermochemical energy storage and considering the requirements listed above.

2 Materials and method

2.1 Materials

The three salts were synthesized using high purity compounds purchased from Merck: Na_2SO_4 ($\geq 99.0\%$), MgSO_4 ($\geq 98.0\%$), LiCl ($\geq 99.0\%$), KCl ($\geq 99.5\%$), $\text{MgCl}_2 \cdot 6\text{H}_2\text{O}$ (99.0-101.0%). The reagents were used directly from their containers without any pre-treatment.

2.2 Salt synthesis methodology

The astrakanite sample was synthesized following the procedure described in [16] which is established based on the phase diagram that is usually applied for leaching solutions from caliche [17]. A mixture of 18.18 wt.% of Na_2SO_4 , 16 wt.% MgSO_4 and 66 wt.% distilled water was prepared at room temperature and heated up to 50 °C. The temperature was kept at 50°C to evaporate the water 150 g of astrakanite was obtained.

The potassium carnallite was synthesized in a glass jacketed reactor of 500 cm³, connected to a thermostatic bath at 35 °C. First, 147 g of distilled water at 35°C was added to 226 g $\text{MgCl}_2 \cdot 6\text{H}_2\text{O}$. Once magnesium chloride hexahydrate was dissolved, 15 g of KCl was gradually added by keeping vigorous stirring with a magnetic bar, during all this stage, the temperature was kept constant at 35°C. After the verification of the complete dissolution of salts, the aqueous solution was transferred from the reactor to a pyrex glass plate. The plate containing the saturated solution was taken into an oven where isothermal evaporation of 64.2 g of water at 35°C took place. Next, the precipitate was separated by filtration under vacuum. Finally, the salt obtained was washed with acetone and as a result, 150 g of potassium carnallite was obtained.

The synthesis process of lithium carnallite was carried out at 30°C. First, 28 g $\text{MgCl}_2 \cdot 6\text{H}_2\text{O}$ and 24 g of LiCl were mixed and grinded in glass mortar. This homogenous mixture was added to glass jacketed reactor containing 28 g of distilled water (previously heated up at 30°C). The resulting solution was transferred to a hermetically sealed glass container, which was taken into a thermostatic shaking water bath during 7 days. After that, the precipitate was separated by vacuum filtration. Finally, the salt crystals were rinsed with acetone. As a result, 50 g of potassium carnallite was obtained.

All products were stored in a desiccator containing silica for future measurements.

2.3 Characterization methods

2.3.1. Chemical Analysis

Sodium, potassium, lithium and magnesium concentration were determined by atomic absorption spectrometry. Chloride and sulfate were determined by volumetric titration with AgNO_3 and BaCl_2 , respectively. Moisture was determined drying the samples until constant weight at 40°C . Based on the results of the chemical analysis, a mineralization to determine the purity of the salts after the drying and washing process with acetone was carried out.

2.3.2 Scanning electron microscope – energy dispersive X-Ray analysis (SEM-EDX)

An scanning electron microscope (SEM) Jeol, Model JSM6360LV was used for analyzing the morphology and composition of the synthesized double-salt hydrates, coupled to an energy dispersive X-ray spectrometer (EDX) Inca Oxford. The measurements were performed under low vacuum, an electron beam of 20 kV, work distance of 10 mm, spot size 60 mm, and backscattered electron signal.

2.3.3. Thermogravimetric – Mass Spectroscopy (TG-MS) analysis

The mass loss curves were recorded by the Thermo-gravimetric (TG) analyzer (TG-SDTA 851e, Mettler Toledo, Spain). The furnace temperature increased from room temperature 25°C to 950°C with heating rate of 5K/min . The flow rate of sweeping nitrogen gas was kept at 50.0 mL/min for all experiments. This flow rate is high enough to sweep the generated gases to avoid changing the local gas environment around the sample. Mass spectroscopy (MS) equipment (Pfeiffer Vacuum ThermoStar, Spain) was coupled with the TG analyzer to track the evolution of volatile products from the TG furnace. The mass of each sample was 49.70 mg , 55.89 mg and 54.37 mg for astrakanite, lithium carnallite and potassium carnallite, respectively. After heating, sulfate and chloride salts could present physical transformations such as, fusion, dehydration or thermal hydrolysis. With respect to the latter, HCl and H_2SO_4 could produce, the hazardousness of which limits the application of salts containing chloride and sulfate hydrates, as TES materials. Because of this, the TG-MS analysis for carnallites and astrakanite was performed to establish the limit temperature for their potential application.

2.3.4. Cycling stability, c_p and dehydration studies

Cycling stability analysis was determined with TGA/DSC Mettler Toledo, in a temperature range of 25°C to 900°C . The heating rate used was 0.5 K/min under N_2 atmosphere, and with a flow rate of 30 mL/min . Standard alumina pan with lid ($40\text{ }\mu\text{L}$) were used.

To determine the phase change temperatures, the latent enthalpy of fusion, c_p values and dehydration studies a DSC 204 F1 Netzsch with N₂ atmosphere (volumetric flow 20 mL/min) was used with crucibles of alumina with 25 μ L volume capacity and with a heat rate of 5 K/min.

2.3.5. Room and High Temperature X-Ray Diffraction (HT-XRD)

Room temperature and high-temperature X-Ray diffraction was performed with PANalytical X'Pert Pro MPD equipment coupled with Anton Paar 1200 HTK oven. In this study, the following measurement conditions were used: 45kVx40mA; static air atmosphere, heating/cooling rate of 5 K/min, radiation of Cu K α 1 ($\lambda=1.5406$ Å); Scan Range: 10–70° in 2 θ ; Step Size: 0.013°. The powdered samples were positioned on a flat plate alumina sample holder after sample powdering. Based on experimental diffractograms the identification of crystallographic phases has been performed by searching the basis of crystal structures: ICDD PDF-2 (version 2004), PAN ICSD (version 2010) and PAN COD (2014 edition).

3 Results

3.1. Chemical characterization

The chemical characterization was carried out to ensure that the synthesized compounds are the expected ones. Chemical analysis, XRD and SEM-EDX were used as identification techniques and the results are shown in Table 1, Table 2 and Figure 1 respectively.

Table 1 Chemical analyses of compounds, in wt. %

Compounds/ Elements	Li	Na	K	Mg	SO ₄	Cl	H ₂ O
Na ₂ SO ₄ ·MgSO ₄ ·4H ₂ O	-	14.16	-	7.12	57.72	-	21.12
KCl·MgCl ₂ ·6H ₂ O	-	-	13.51	8.89	-	38.16	39.52
LiCl·MgCl ₂ ·7H ₂ O	2.67	-	-	9.04	-	39.52	48.73

The results of mineralization indicated that both potassium and lithium carnallites have a purity of 96-98% (dry solids without impregnation) and some non-identified impurities. Regarding astrakanite mineralization, the results indicate that it is associated with loweite (Na₂SO₄·MgSO₄·2,75H₂O). To identify impurities, diffraction has been performed and the results are summarized in the Table 2.

Table 2 Summary of phases identified by XRD and mineralization wt. %

Sample	Main mineral phase	Impurities
$\text{Na}_2\text{SO}_4 \cdot \text{MgSO}_4 \cdot 4\text{H}_2\text{O}$	Astrakanite (95%)	Loweite (<3%) and other non-identified phases
$\text{KCl} \cdot \text{MgCl}_2 \cdot 6\text{H}_2\text{O}$	Potassium Carnallite (96%)	Bischofite (<4%)
$\text{LiCl} \cdot \text{MgCl}_2 \cdot 7\text{H}_2\text{O}$	Lithium Carnallite (98%)	Non-identified impurities (~2%)

XRD results confirm the formation of double salts. For astrakanite provides that with this salt loweite is formed, a compound having the same composition, but fewer molecules of water of crystallization. For potassium carnallite, it was established that there is unreacted magnesium chloride hexahydrate. For lithium carnallite, no mineral phase of impurities could be established, probably because they are not found in the database.

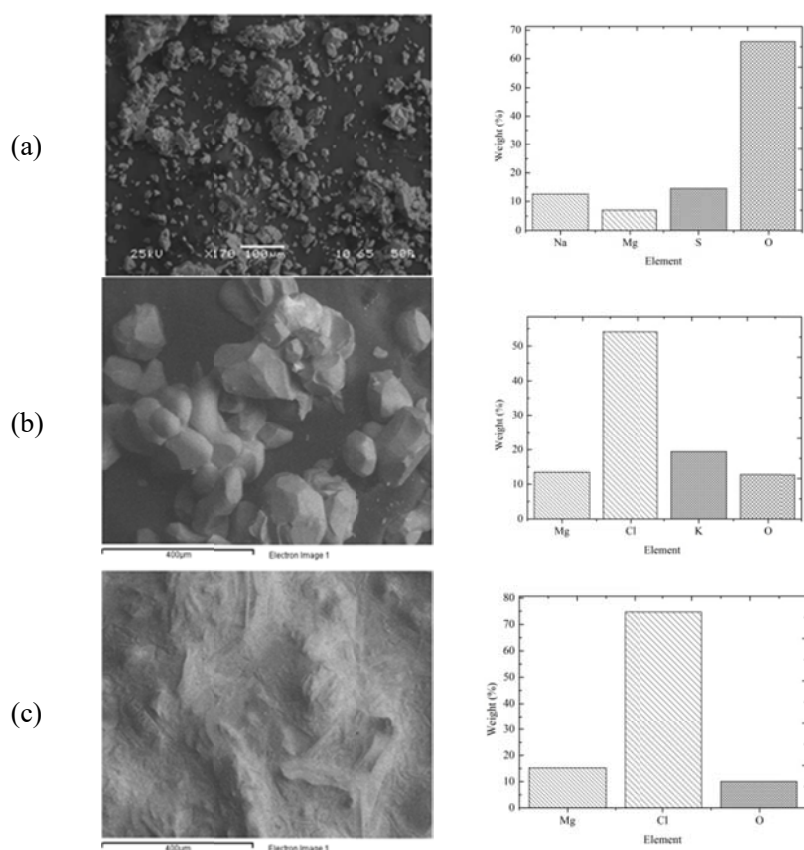


Figure 1 SEM image (on the left side) and composition based on EDX (on the right side) for (a) astrakanite [16], (b) potassium carnallite and (c) lithium carnallite.

As seen in Figure 1 (a) astrakanite and (b) potassium carnallite show separated and well defined crystals. In the case of (c) lithium carnallite, as this salt has a strong hygroscopic behavior absorbs humidity from the atmosphere so that, it looks like agglomerate material where is not possible to see individual and well defined crystals. The composition obtained by EDX analysis (plot on the right side of each sample) show the mass percent of elements, presented in double salts under study. It will be notice that the absence of lithium wt.% on chemical composition for $\text{LiCl} \cdot \text{MgCl}_2 \cdot 7\text{H}_2\text{O}$ is explained by the limitation of SEM-EDX to quantify this element.

3.2. Thermal characterization

3.2.1. Astrakanite

- Dehydration studies of astrakanite

The DSC curve for the dehydration process of astrakanite is shown in Figure 2. This process starts at 110.6 °C, presenting two peaks at 121.3 °C and at 130.8 °C, up to about 225 °C, where the dehydration process finishes. The enthalpy of dehydration for the complete process is significantly high, 506.2 J/g. This high amount of energy involved in the dehydration process makes it promising to be applied as a TCM at medium temperature, if this dehydration reaction is reversible. To confirm this condition further studies are required.

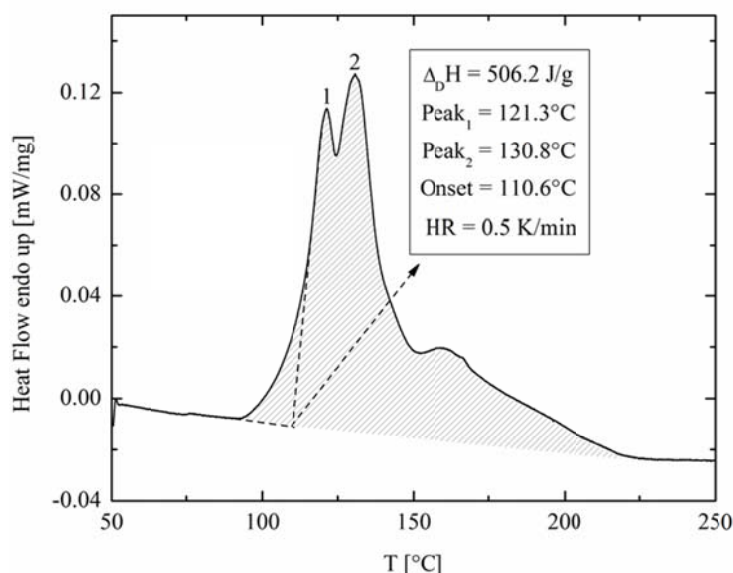


Figure 2 Dehydration study of astrakanite

Since astrakanite is a “unimolar” double hydrated sulfate salt of $\text{Na}_2\text{SO}_4 \cdot \text{MgSO}_4 \cdot 4\text{H}_2\text{O}$, once dehydrated, it becomes a mixture of those salt sulfates at 50% molar composition of each one. This product, obtained from dehydration of synthetic astrakanite was analyzed for two heating and cooling cycles. The DSC curves are show in Figure 3.

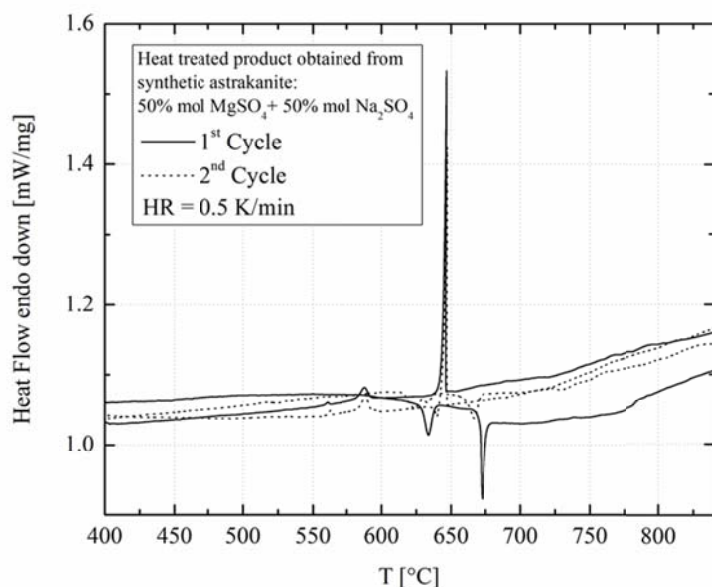


Figure 3 DSC curves of two cycles of heating and cooling for heat treated product coming from synthetic astrakanite [16]

Results of DSC measurements clear up that the melting and solidification processes took place in two steps, with two peaks for each process. The values of temperatures and enthalpies, involved in each cycle are summarized in Table 3.

Table 3 Summary of T° , $\Delta_F H$, $\Delta_S H$ for dehydrated astrakanite

Cycle		First peak		Second peak	
		T_{onset} , °C	$\Delta_F H$, J/g	T_{onset} , °C	$\Delta_S H$, J/g
1	Heating	628.6	35.6	671.0	58.5
	Cooling	646.1	88.5	592.0	28.3
2	Heating	615.9	34.8	660.2	35.4
	Cooling	646.8	85.3	592.0	30.6

The two peaks in the DSC curves indicate that the binary mixture melts in two steps. Even though this mixture has an equimolar composition, 50% mol MgSO_4 + 50% mol Na_2SO_4 , the two peaks show that it might not correspond to an eutectic point. Two studies reported theoretical phase diagrams for the system MgSO_4 - Na_2SO_4 . Each phase diagram shows different composition for the

eutectic point of this binary system. The first study reports a molar composition of 45.2% mol MgSO_4 + 54.8% mol Na_2SO_4 (eutectic mixture 1), presented by Bandaranayake and Mellander [18]. The second study reports a molar composition of 48% mol MgSO_4 + 52% mol Na_2SO_4 (eutectic mixture 2), presented by Du [19] (see Figure 4).

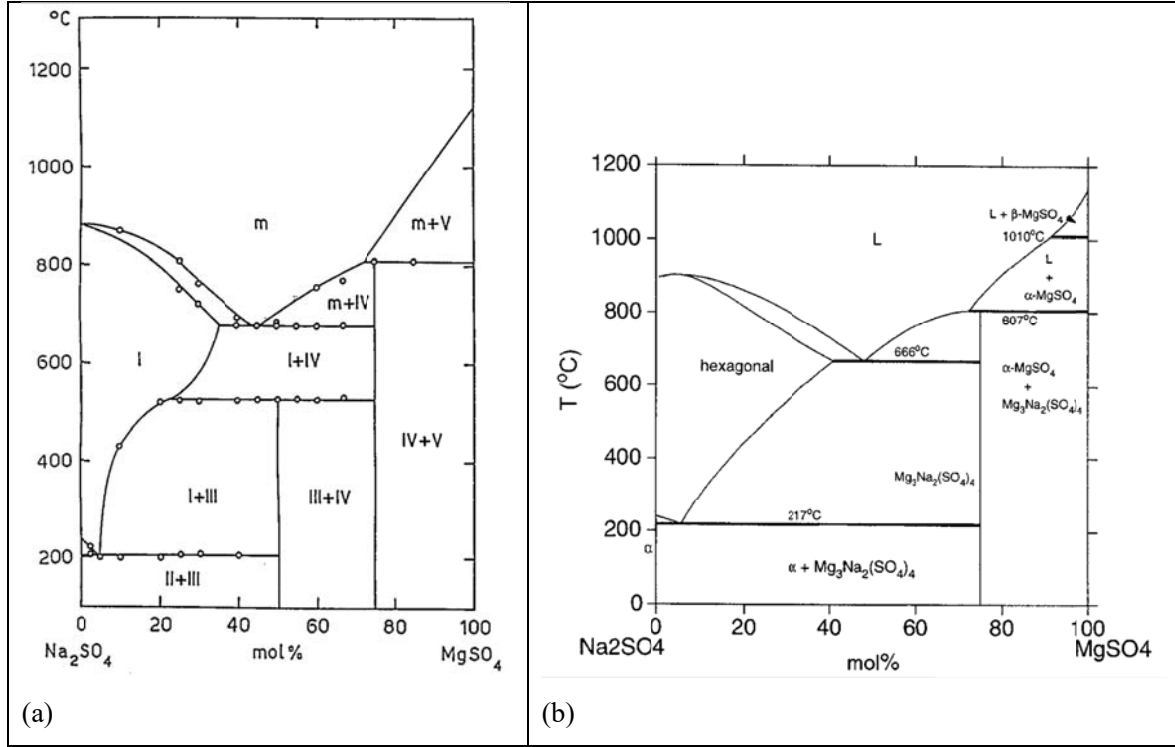


Figure 4. Binary phase diagrams a) for eutectic mixture 1 [18] and b) eutectic mixture 2 [19]

In order to establish the use of astrakanite as low cost material in the preparation of eutectic mixtures and future used as PCM, these two eutectic compositions were tested.

Two cycles of heating and cooling were performed for the eutectic mixture 1, and the curves of DSC analysis are shown in Figure 5 (a). The melting process of the first cycle (continuous line) occurs in one step, at $T_{\text{onset}} = 671.2$ °C and $\Delta_f H = 105.0$ J/g, as well as the crystallization process, at $T_{\text{onset}} = 640.3$ °C and $\Delta_s H = 129.0$ J/g. However, during the second cycle (dotted line), the melting process occurs in two steps. The first step occurs at $T_{\text{onset}}^1 = 639.5$ °C and $\Delta_f H^1 = 38.8$ J/g, and the second step occurs at $T_{\text{onset}}^2 = 662.2$ °C and $\Delta_f H^2 = 51.7$ J/g. Finally, the crystallization process of the second cycle occurs similarly than the first cycle, in only one step at $T_{\text{onset}} = 637.8$ °C and $\Delta_s H = 123.4$ J/g.

The same as the eutectic mixture 1, the curves of DSC analysis of two cycles of heating and cooling are shown in Figure 5 (b).

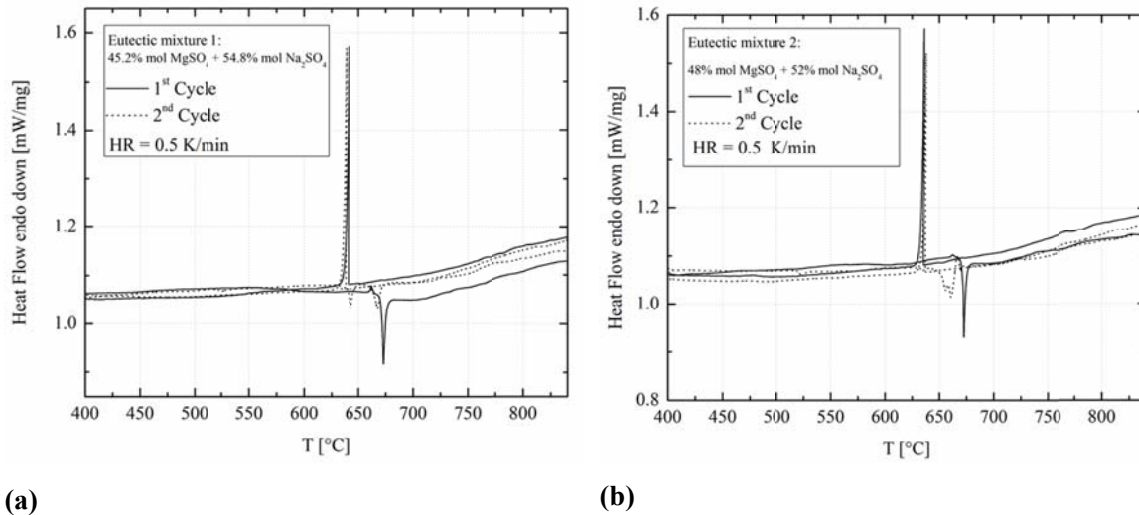


Figure 5 DSC studies of two cycles of heating and cooling for a) eutectic mixture 1 [18] and b) eutectic mixture 2 [19]

Compare to the eutectic mixture 1, this one shows a more stable behavior, since the first cycle of heating and cooling (continuous line) occurs in one step, as well as the second cycle (dotted line). The values for the cycle are: first heating, $T_{\text{onset}} = 671.6 \text{ }^{\circ}\text{C}$ and $\Delta_{\text{F}}H = 85.7 \text{ J/g}$ and first cooling, $T_{\text{onset}} = 635.3 \text{ }^{\circ}\text{C}$ and $\Delta_{\text{S}}H = 119.8.7 \text{ J/g}$. Likewise, the second heating, $T_{\text{onset}} = 655.9 \text{ }^{\circ}\text{C}$ and $\Delta_{\text{F}}H = 103.1 \text{ J/g}$ and second cooling, $T_{\text{onset}} = 637.1 \text{ }^{\circ}\text{C}$ and $\Delta_{\text{S}}H = 111.1 \text{ J/g}$.

This eutectic mixture 2 shows also better performance than the eutectic mixture obtained as a product of heat treatment of astrakanite (see Figure 3). Not only because the melting and crystallization processes occur in one step, but also because the potential enthalpy of fusion and solidification, above 100 J/g, are promising for this material can be applied as a PCM at high temperature.

- TG-MS of astrakanite

In order to gain more insight into the thermal degradation process, and to monitor the signals of some of the potential gases such as SO_x , evolved in thermal decomposition of astrakanite, thermogravimetric (TG) analyses coupled with a mass spectrometer (MS) experiments were performed. Results show that the main signal corresponds to mass 18, which according to composition of astrakanite indicates the releasing of water (see Figure 6). No other signal was observed in the results of TG-MS, this means that the dehydration process of astrakanite is finished by 300°C , releasing only water vapor. Dehydrated product of astrakanite, obtained after 300°C , and corresponding to the binary equimolar mixture is a very stable material, because no signal with mass 64 (MW SO_2) is observed up to 900°C . That means no SO_2 is released.

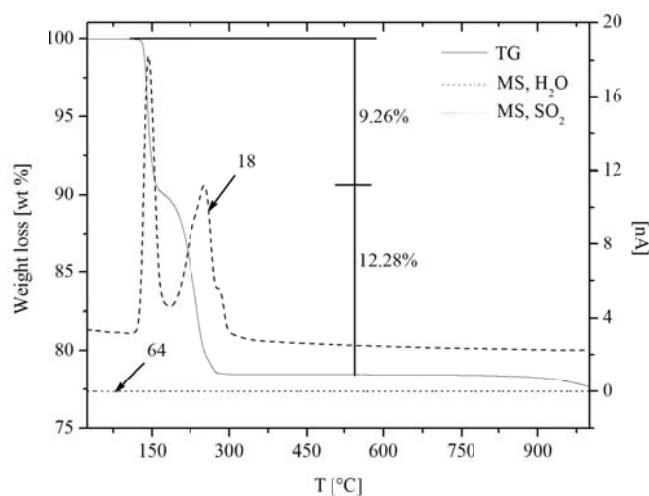


Figure 6 TG-MS curves of astrakanite

- HT – XRD of astrakanite

The results for two cycles of heating and cooling, in a temperature range from 25°C to 550°C, of astrakanite by HT-XRD are shown in Figure 7. A transition phase is observed during the first heating step (25 - 300 °C), which corresponds to dehydration process and water loss. At 300°C, the formation of new crystalline phase is observed and, based on TG-MS and DSC studies correspond to binary equimolar mixture. This new phase remains stable during the cooling step of the first cycle and during the whole second heating/cooling cycle.

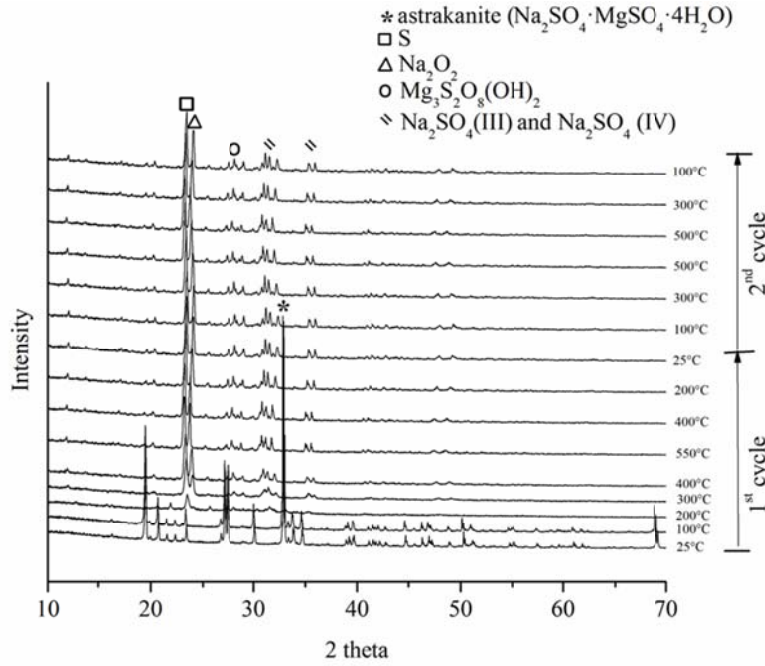


Figure 7 HT-DRX diffractograms for two cycles of heating/ cooling of astrakanite

It is remarkable that the material does not change its phase, remaining a stable solid phase during both cycles of heating/cooling.

Additionally, c_p measurements for the solid phase, equimolar mixture 50%mol MgSO_4 + 50% mol Na_2SO_4 , were performed and the results are summarized in Figure 8.

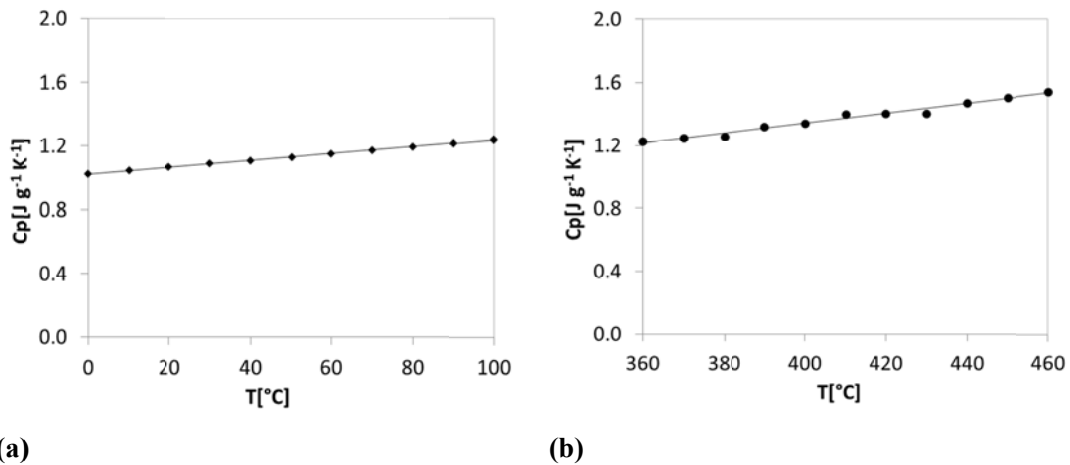


Figure 8 c_p measurements for astrakanite (a) and dehydrated product, corresponding to the binary equimolar mixture (b)

As can be seen from Figure 8, the c_p results have a linear behavior with temperature for both samples and have the values compared with solid sensible heat storage materials [15].

3.2.2. Potassium carnallite

The dehydration process of potassium carnallite takes place in two separate steps as it is shown in Figure 9. The first step starts at 84.2 °C with an enthalpy of dehydration of 683.3 J/g. The second step starts at 127.1 °C and the enthalpy of dehydration is 330.4 J/g. As well as astrakanite, if this dehydration reaction is reversible, the potential of potassium carnallite to be applied as TCM at medium temperature is significant, due to the high amount of energy involved in this process.

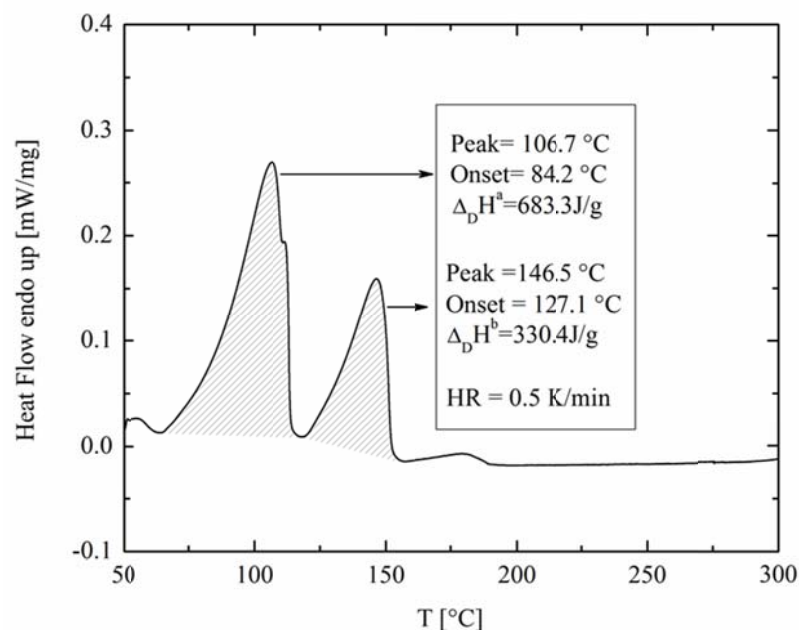


Figure 9 Dehydration studies of potassium carnallite

- TG-MS studies of potassium carnallite

In order to confirm the thermal behavior of potassium carnallite and to characterize the gaseous product of decomposition, TG-MS was carried out up to 1000°C. Results are summarized on Figure 10. The results show that the main signal corresponds to mass 18. Just as astrakanite, this indicates the releasing of water molecules in two steps. The temperatures corresponding to each step are higher than those obtained from DSC measurements. This results from the fact that the heating rate used for the DSC measurements is 10 times slower. That said, even when the amount of sample is small, it has more time to increase its temperature and release the water of crystallization contained in the structure of potassium carnallite. Additionally, a weak signal corresponding to 36 (MW HCl) indicates the presence of HCl at 250°C and at 450°C (see Figure 10 (a)). Also, a slight upward curve from 500°C to 1000°C, are observed, which means that the most significant releasing of HCl takes place at this range of temperature. It is important to highlight, that the release of HCl takes

place due to the decomposition of potassium carnallite, as well as the decomposition of bischofite that is present as impurity in the sample.

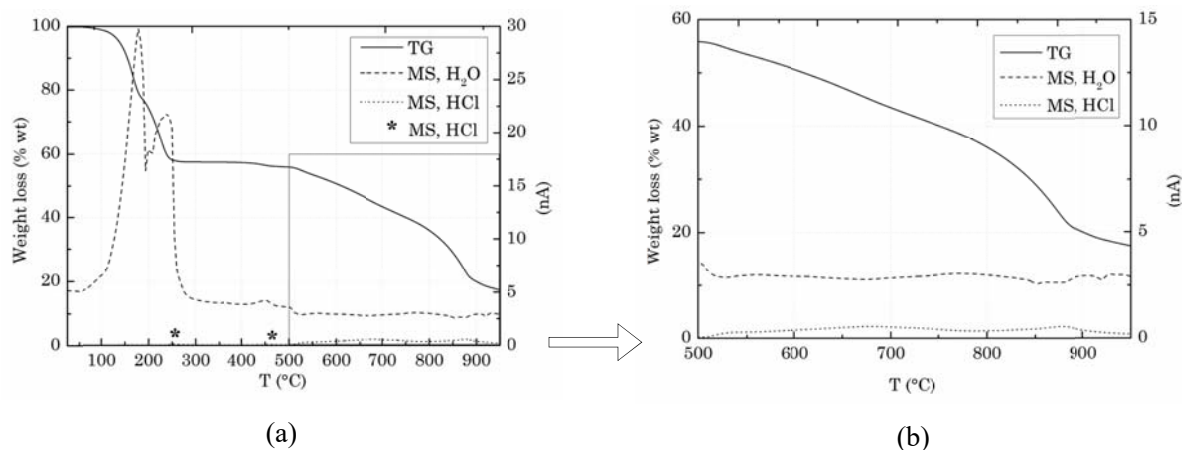


Figure 10 TG-MS of potassium carnallite until 1000 °C

Based on the results of thermal behavior, it can be stated the presence of a stable product within the range of temperature from 240°C to 440°C.

- HT – XRD of potassium carnallite

To confirm the stability of potassium carnallite, X-ray diffraction measurements were performed at high temperature, from 25°C to 400°C. The results obtained are shown in Figure 11.

According to these results combined with those obtained from TG measurements, the release of H₂O and HCl take place up to 280°C. Above this temperature, at 300°C and 400°C can be detected the formation of a different crystalline phase, however, both are different between each other. These results indicate that even when there is no release of gases, several solid-solid transformations take place in the sample. As a consequence, it is not possible to apply the heat treated product obtained from potassium carnallite as a sensible TES material.

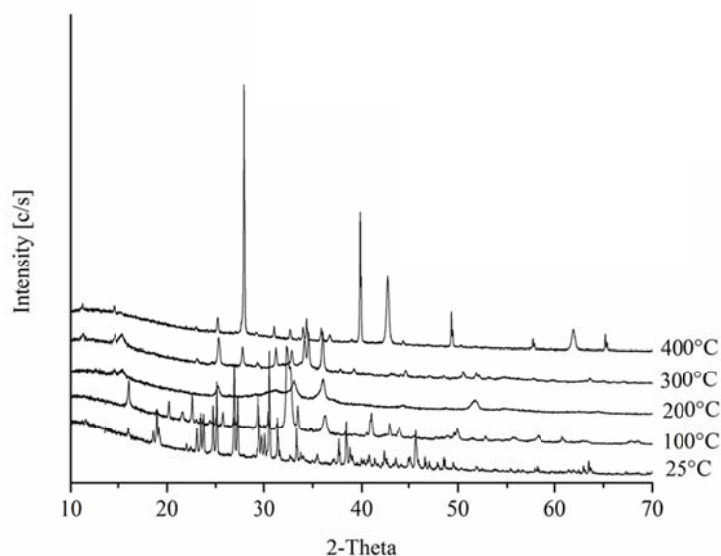


Figure 11 HT-DRX diffractograms of potassium carnallite and their products after dehydration

3.2.3. Lithium canallite ($\text{LiCl} \cdot \text{MgCl}_2 \cdot 7\text{H}_2\text{O}$)

- TG-MS of lithium carnallite

Just like potassium carnallite, lithium carnallite is also a salt hydrate composed by magnesium and chloride, besides of lithium. This is the reason why the releasing of HCl was also monitored, while the temperature was increasing. Figure 12 shows the resulting curves obtained from the analysis. Similarly than potassium carnallite, results show that the main signal corresponds also to mass 18, indicating the releasing of water. In the same way, the signal corresponding to 36 (MW HCl), at 250°C and at 450°C, indicates the releasing of HCl in small amounts. Additionally, a continuous and more significant signal appears from 600°C to 900°C, 100°C higher than for potassium carnallite, indicating that a most significant releasing of HCl takes place at this range of temperature.

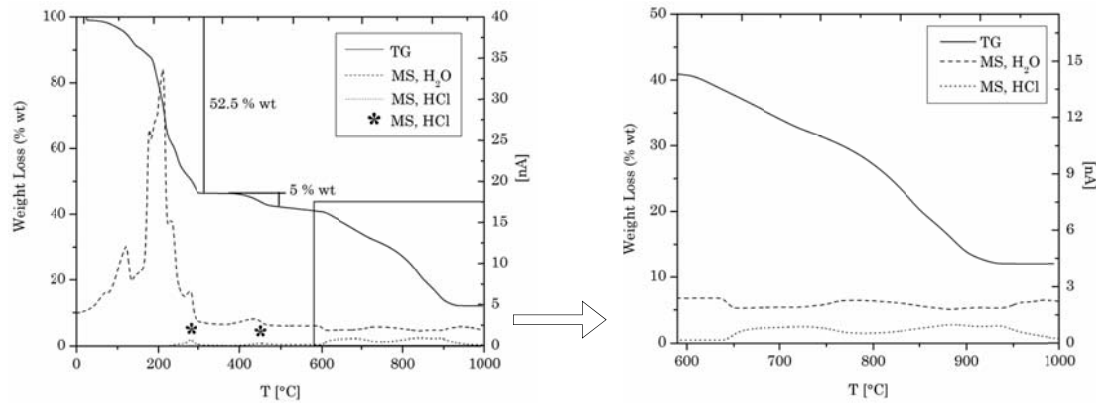


Figure 12 TG-MS for lithium carnallite.

The curves obtained for the three cycles of heating and cooling by DSC method for lithium carnallite are shown in Figure 13. It can be observed three curves of melting and two curves of solidification process. The first solidification peak cannot be observed because this material does not solidify during the cooling process, but it does during the isotherm stage between the two cycles at 40°C during 20 min.

The results obtained for the three cycles are listed as follows:

- 1st cycle, melting process: $T_{\text{onset}} = 92.1^{\circ}\text{C}$ and $\Delta_{\text{F}}H = 62.9 \text{ J/g}$.
- 1st cycle, solidification process: not available as was mentioned before.
- 2nd cycle, melting process: $T_{\text{onset}} = 91.4^{\circ}\text{C}$ and $\Delta_{\text{F}}H = 61.2 \text{ J/g}$.
- 2nd cycle, solidification process takes place in two stages:
 $T_{\text{onset}}^1 = 43.7^{\circ}\text{C}$ and $\Delta_{\text{C}}H^1 = 60.2 \text{ J/g}$ and $T_{\text{onset}}^2 = 42.6^{\circ}\text{C}$ and $\Delta_{\text{C}}H^2 = 8.6 \text{ J/g}$
- 3rd cycle, melting process: $T_{\text{onset}} = 84.3^{\circ}\text{C}$ and $\Delta_{\text{F}}H = 24.4 \text{ J/g}$.
- 3rd cycle, solidification process also takes place in two stages:
 $T_{\text{onset}}^1 = 44.8^{\circ}\text{C}$ and $\Delta_{\text{C}}H^1 = 59.6 \text{ J/g}$ and $T_{\text{onset}}^2 = 43.5^{\circ}\text{C}$ and $\Delta_{\text{C}}H^2 = 9.3 \text{ J/g}$

It can be seen that as many successive cycles of heating and cooling are performed, the thermal properties of this material are changing as well. This may indicate that lithium carnallite not only melts and solidifies during cycles but also decomposes simultaneously.

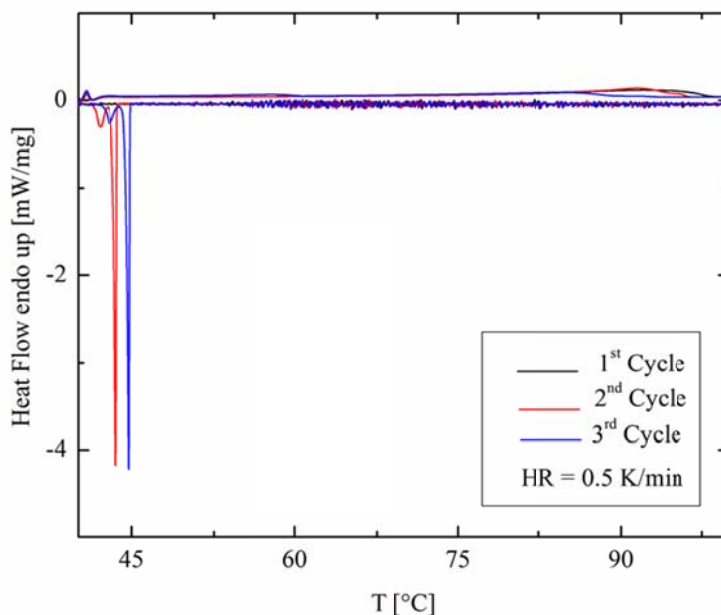


Figure 13 DSC cycle studies of lithium carnallite

Results from TG-MS combined with those obtained from DSC measurements confirmed that lithium carnallite starts to loss mass at 80°C due to the release of H₂O and it melts simultaneously. It is also possible to observe significant subcooling of about 40°C. As a consequence, lithium carnallite in the present form is not promising to be applied as TES material, either latent or sensible heat storage media.

4 Discussion

Based on the requirements for TES materials previously mentioned and results showed in this study, Table 4 lists and summarizes the materials under study and the characterization results. Moreover, their potential to be used as sensible TES materials, PCM, and TCM are also highlighted in this table. Notice that astrakanite can be used in their hydrated and anhydrous forms. Astrakanite and Na₂SO₄·MgSO₄ (dehydrated product from astrakanite), are potential candidates to be used as sensible TES materials due to their thermal stability and proper c_p values. Moreover, eutectic mixtures such as 54.5 wt. % Na₂SO₄ + 45.5 wt. % MgSO₄, and 52 wt. % Na₂SO₄ + 48 wt. % MgSO₄ are suitable candidates with potential to be used as PCM at high temperature because of their enthalpies of phase change. Furthermore, the results of TG-MS and DSC performed for astrakanite and potassium carnallite show the releasing of water below 300°C. The dehydration mechanism and temperature of astrakanite show close concordance with results obtained by Balik-

Zunic et al. [19]. Additionally, astrakanite and carnallite require high specific energy for dehydration, based on this; both materials have potential to be applied as TCM. Although further studies need to be performed in order to demonstrate the reversibility of dehydration/hydration reactions. Finally, the studies performed for lithium carnallite, show that this material is not promising as TES material due to its ambiguous behavior, presenting phase change and weight loss (decomposition) simultaneously at low temperature.

Table 4 Materials under study and summary of characterization results.

	Sensible TES materials candidates		PCM candidates		TCM candidates			
Compound	c_p [J/g·K]	Range of temperature [°C]	$\Delta_f H$ [J/g]	T_{onset} [°C]	$\Delta_D H$ [J/g] and reaction kinetics	T_{onset} [°C]	Chemical stability	
							TG-MS	HT-XRD
Astrakanite ($Na_2SO_4 \cdot MgSO_4 \cdot 4H_2O$)	1.022-1.242	0-100	---	---	506.2	110.6 TG-MS T_{peak1} : 135°C T_{peak2} : 253°C	No SO_2 release up to 900 °C 9.26 wt.% loss of H_2O up to 150 °C + 12.28 wt. % loss of H_2O up to 300 °C	Changing crystalline structure up to 300°C
$Na_2SO_4 \cdot MgSO_4$ dehydrated product obtained from astrakanite	1.225-1.537	360-460	---	---	---	---	---	New phase obtained remains stable with temperature
Eutectic 1: 54.5 wt.% Na_2SO_4 + 45.5 wt.% $MgSO_4$	---		1 st heating: 105.0	671.2	---	---	---	---
			2 nd heating in two steps: 38.8 and 51.7	639.5 and 662.2		---	---	---
Eutectic 2: 52 wt.% Na_2SO_4 + 48 wt.% $MgSO_4$	---		1 st heating: 85.7	671.6	---	---	---	---
	---	---	2 nd heating: 103.1	655.9	---	---	---	---

Potassium carnallite (KCl·MgCl ₂ ·6H ₂ O)	---		---		Peak 1: 683	84.2	HCl release in range 250°C and starting continuous release at 475 °C	Changing crystalline structure with temperature
		---			Peak 2: 330	127.1	20.5 wt.% loss of H ₂ O up to 110 °C +22.3 wt. % loss of H ₂ O and HCl up to 160 °C	
		---					No Cl ₂ released	
Lithium carnallite (LiCl·MgCl ₂ ·7H ₂ O)	---	---	---	---	---	---	52.5 wt.% loss (calc. 47.8wt.% of H ₂ O and 4.7 wt.% of HCl) up to 300 °C)	
		---		---		---	HCl release in range 240-300°C, 400-500°C (5 wt. %) and starting continuous release at 590 °C (30.5 wt. %)	
		---		---		---	No Cl ₂ released	

5 Conclusions

Based on the thermophysical characterization of three double salt hydrates, astrakanite, potassium carnallite and lithium carnallite the conclusions are listed below.

Astrakanite has potential to be applied as TCM at low-medium temperature. The dehydrated binary mixture obtained from astrakanite is promising as PCM at high temperature, due to its binary composition is close to the eutectic point. In addition, to support these results, the binary eutectic mixtures of sulfates were evaluated showing promising results as potential high temperature PCM as well. Potassium carnallite has potential to be applied as TCM at low-medium temperature, however deep and detailed studies need to be performed.

Lithium carnallite has no potential to be applied as TES material under the conditions performed in this study.

Acknowledgements

The work at the University of Antofagasta was supported by CONICYT/FONDAP N° 15110019 and ERANet-LAC 2nd Joint Call, ERANET-LAC 2015-2016, project ELAC2015/T06-0988. The authors from the University of Lleida and the University of Barcelona would like to thank the Catalan Government for the quality accreditation given to their research group GREA (2014 SGR 123) and DIOPMA (2014 SGR 1543), respectively. The work was partially funded by the Spanish government (ENE2015-64117-C5-1-R (MINECO/FEDER)). This project has received funding from the European Commission Seventh Framework Programme (FP/2007-2013) under Grant agreement N°PIRSES-GA-2013-610692 (INNOSTORAGE) and from the European Union's Horizon 2020 research and innovation programme under grant agreement No 657466 (INPATH-TES). Dr. Camila Barreneche would like to thank Ministerio de Economía y Competitividad de España for grant Juan de la Cierva, FJCI-2014-22886.

References

- [1] H. Mehling, L.F. Cabeza, Heat and cold storage with PCM: An up to date introduction into basics and applications, Springer-Verlag Berlin Heidelberg, 2008.
- [2] A. Abhat, Low temperature latent heat thermal energy storage: heat storage materials. Sol. Energy 30 (1983) 313–332.
- [3] L.F. Cabeza, Advances in thermal energy storage systems: Methods and applications Woodhead Publishing, 2014.
- [4] A. I. Fernández, M. Martínez, M. Segarra, I. Martorell, L.F. Cabeza, Selection of materials with potential in sensible thermal energy storage, Sol. Energ. Mat. Sol. C. 94 (2010) 1723 - 1729.

- [5] L.F. Cabeza, , A. Castell, C. Barreneche, A. De Gracia, A.I. Fernández, Materials used as PCM in thermal energy storage in buildings: A review, *Renew. Sust. Energ. Rev.* 15 (2011) 1675-1695.
- [6] M. Kenisarin and K. Mahkamov, Sal Hydrates as Latent heat storage materials: Thermophysical properties and costs, *Sol. Energ. Mat. Sol. C.* 145 (2016) 255 – 286.
- [7] C. Barreneche, M. E. Navarro, L. F. Cabeza, A. I. Fernández, New database to select phase change materials: Chemical nature, properties, and applications, *Journal of Energy Storage* 3 (2015) 18–24.
- [8] A. Solé, X. Fontanet, C. Barreneche, A. I. Fernández, I. Martorell, Luisa F. Cabeza, Requirements to consider when choosing a thermochemical material for solar energy storage, *Sol. Energy* 97 (2013) 398-404.
- [9] Obermeier, K. Müller, W. Arlt, Thermodynamic analysis of chemical heat pumps, *Energy* 88 (2015) 489-496.
- [10] G. Whiting, D. Grondin, S. Bennici, A. Auroux, Heat of Water sorption studies on zeolite-MgSO₄ composites as potential thermochemical heat storage materials, *Sol. Energ. Mat. Sol. C.* 112 (2013) 112 – 119.
- [11] A.H. Abedin and M.A. Rosen, A Critical Review of Thermochemical Energy Storage Systems, *Open Renewable Energy Journal*, 4 (2011) 42-46.
- [12] A. Gutierrez, A. Gil, J. Rodríguez-Aseguinolaza, C. Barreneche, N. Calvet, X. Py, A. I. Fernández, M. Grágeda, S. Ushak, L.F. Cabeza, Review on industrial waste and by-product materials revalorization as thermal energy storage (TES) materials, *Renew. Sust. Energ. Rev.*, 59 (2013) 763 – 783.
- [13] Anuario de la Minería de Chile, <http://www.sernageomin.cl/pdf/mineria/estadisticas/anuario/anuario2013.pdf>, 2013 (accessed 22.09.2016)
- [14] S. Ushak, A. Gutierrez, H. Galleguillos, A.G. Fernandez, L.F. Cabeza, M. Grágeda, Thermophysical characterization of a by-product from the non-metallic industry as inorganic PCM, *Sol. Energ. Mat. Sol. C.* 132 (2015) 385–391.
- [15] M.E. Navarro, M. Martínez, A. Gil, A.I. Fernández, L.F. Cabeza, R. Olives, X. Py, Selection and characterization of recycled materials for sensible thermal energy storage, *Sol. Energ. Mat. Sol. C.* 107, 2012, 131–135.
- [16] S. Ushak, A. Gutierrez, E. Flores, H. Galleguillos, M. Grágeda, Development of Thermal Energy Storage Materials from Waste-Process Salts, *Energy Procedia* 5 (2014) 627 – 632.

- [17] S. Ushak, A. Gutierrez, Y. Galazutdinova, C. Barreneche, L.F. Cabeza, M. Grágeda, Influence of alkaline chlorides on thermal energy storage properties of bischofite, *Int. J. Energy Res.* 40 (2016) 1556 – 1563.
- [18] P.W.S.K. Bandarayake and B.E. Mellander, Phase transitions and ionic conductivity of the Na₂SO₄ – MgSO₄ System, *Solid State Ionics* 40/41 (1990) 31-33.
- [19] H. Du, Thermodynamic assessment of the K₂SO₄ – Na₂SO₄ – MgSO₄ – CaSO₄ System, *J. Phase Equilib.* 21 (2000) 6 -18.
- [20] T. Balic-Zunic, R. Birkedal, A. Katerinopoulou, P. Comodi, Dehydration of bloedite, Na₂Mg(SO₄)₂(H₂O)₄, and leonite, K₂Mg(SO₄)₂(H₂O)₄, *Eur. J. Mineral*, 28 (2016) 33-42.